Generation and analysis of typical meteorological years for future weather and detection of heatwaves

Qian, Bin; Zhang, Chen; Heiselberg, Per; Yu, Tao; Jønsson, Kim Trangbæk

Publication date:
2021

Document Version
Publisher's PDF, also known as Version of record

DEPARTMENT OF CIVIL ENGINEERING
AALBORG UNIVERSITY

Generation and Analysis of Typical Meteorological Years for Future Weather and Detection of Heatwaves

Bin Qian
Chen Zhang
Per Kvols Heiselberg
Tao Yu
Kim Trangbæk Jønsson

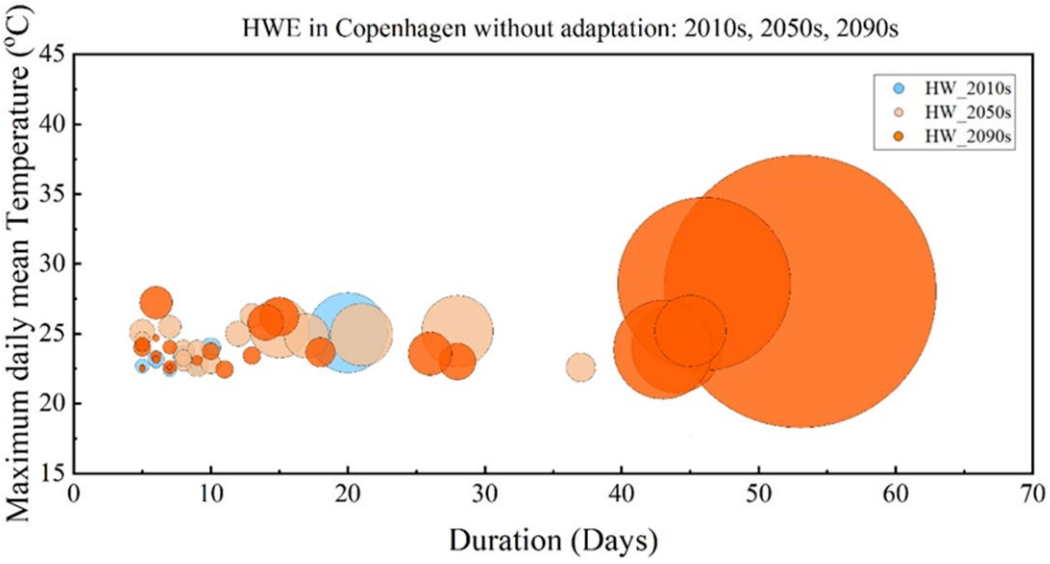

ISSN 1901-726X
DCE Technical Report No. 300

Aalborg University
Department of the Civil Engineering
Division of Sustainability, Energy and Indoor Environment

DCE Technical Report No. 300

Generation and Analysis of Typical Meteorological Years for Future Weather and Detection of Heatwaves

by

Bin Qian
Chen Zhang
Per Kvols Heiselberg
Tao Yu
Kim Trangbæk Jønsson

Dec 2021

Scientific Publications at the Department of Civil Engineering

Technical Reports are published for timely dissemination of research results and scientific work carried out at the Department of Civil Engineering (DCE) at Aalborg University. This medium allows publication of more detailed explanations and results than typically allowed in scientific journals.

Technical Memoranda are produced to enable the preliminary dissemination of scientific work by the personnel of the DCE where such release is deemed to be appropriate. Documents of this kind may be incomplete or temporary versions of papers—or part of continuing work. This should be kept in mind when references are given to publications of this kind.

Contract Reports are produced to report scientific work carried out under contract. Publications of this kind contain confidential matter and are reserved for the sponsors and the DCE. Therefore, Contract Reports are generally not available for public circulation.

Lecture Notes contain material produced by the lecturers at the DCE for educational purposes. This may be scientific notes, lecture books, example problems or manuals for laboratory work, or computer programs developed at the DCE.

Theses are monograms or collections of papers published to report the scientific work carried out at the DCE to obtain a degree as either PhD or Doctor of Technology. The thesis is publicly available after the defence of the degree. Since 2015, Aalborg University Press has published all Ph.D. dissertations in faculty series under the respective faculty. The AAU Ph.D.-portal will host the E-books, where you also find references to all PhDs dissertations published from Aalborg University.

Latest News is published to enable rapid communication of information about scientific work carried out at the DCE. This includes the status of research projects, developments in the laboratories, information about collaborative work and recent research results.

Published 2021 by
Aalborg University
Department of the Built Environment
Thomas Manns Vej 23
DK-9220 Aalborg E, Denmark

Printed in Aalborg at Aalborg University

ISSN 1901-726X
DCE Technical Report No. 300

1. Introduction

With the influence of industrialization, economic development, urban heat island effect, population growth and other factors, climate change is becoming one of the biggest challenges faced by society [1]. Especially, extreme weather events, such as heatwaves, not only have a negative impact on the occupants' thermal comfort but also raise heat-related diseases or even cause death, especially for vulnerable populations [2] [3]. Therefore, it is essential to design buildings and their systems not only for today but also for future weather conditions. Building performance simulation is an important tool to support building design. At present, the weather data used in simulations are generally in form of typical weather years, such as Typical Meteorological Year (TMY), Design Reference Year (DRY) and International Weather for Energy Calculations (IWEC) generated by long-term historical data observed at weather stations [4]. These data are not frequently updated, but are generated as typical year data from the past twenty or thirty years and serve a longer time. The rate of global warming is likely to make these weather data obsolete earlier, with the global mean temperature already increased by around +1.2 °C compared to pre-industrial conditions [5] and expecting to further increase above 2 C before the turn of the century. It becomes important to use future typical weather year data to simulate building energy consumption and thermal environment in order to better predict or evaluate building performance [6] [7].

Furthermore, due to climate change, the frequency, intensity and severity of extreme weather events, such as heatwaves, coldwaves, storms, heavy precipitation causing wildfires, floods, and droughts are increasing, which could adversely affect human health [8]. Extreme temperatures for long periods have enormous adverse social, economic and environmental effects, such as the death of thousands of vulnerable elderly people, the destruction of large areas of forests by fire, and effects on water ecosystems and glaciers during the well-known European heatwave of 2003 [9]. For the thermal environment and energy consumption of buildings, heatwave events will undoubtedly have a considerable impact. The existence of heatwaves will increase the cooling load and energy consumption of active cooling, such as air-conditioning system [10], or reduce the thermal comfort of buildings under passive cooling such as nature ventilation systems [11]. The impact is not easy to detect in TMY and even could be deliberately underestimated when selecting the typical month since the value of extreme weather is far away from the average situation. This means that TMY data alone cannot be used to assess the performance of buildings in extreme weather conditions. The building engineering community has taken measures to assess overheating at the design stage like providing Design Summer Years (DSY) [12], Extreme Meteorological Year (XMY), Hot Summer Year (HSY) for building simulation [4]. In order to assess the resilience cooling performance of buildings under future extreme weather conditions, heatwaves should be considered when preparing future weather data. However, there is no universal definition of heatwave and relevant methods for detecting heat waves are still under discussion. The World Meteorological Organization defines a heatwave as five or more consecutive days of prolonged heat in which the daily maximum temperature is higher than the average maximum temperature by 5 °C or more [13]. However, some nations have come up with their own criteria to define a heatwave. The most common approach is to use fixed temperature thresholds for maximum or/and minimum temperature, where the thresholds vary for different regions. The minimum duration of a heatwave also varies from nation to nation [3]. Some nations define a heatwave with the maximum temperature such as Adelaide and Sweden. In Adelaide, South Australia, a heatwave is defined as five consecutive days at or above 35 °C, or three consecutive days at or over 40 °C [14]. In Sweden, a heatwave is defined as at least five days in a row with a daily high exceeding 25 °C [15]. Some nations also provide minimum temperatures for a heatwave such as Greece, according to the

Hellenic National Meteorological Service, a heatwave is defined as three consecutive days at or above 39 °C and a minimum temperature in the same period at or over 26 °C [16]. In fact, the temperature thresholds might be changed with the possible adaptation of the population to heat [17]. Temperatures that people from a hotter climate consider normal can be called a heatwave in a cooler area if they are outside the normal climate pattern for that area [18].

This study adopts a new method which is suggested by Annex 80. We generated three typical years' weather data for Copenhagen including one historical period and two future periods, and then compared the results with observations and TMYs from Meteonorm software. Heatwave events (HWEs) were detected by using a new definition that used at least three consecutive days average daily temperature in reference historical period to detect HWEs. To consider the thermal adaptation, we also proposed another definition that used the different thresholds to detect HWEs for different periods. . HWEs detected by the above two definitions were compared with those detected by Danish definitions.

2. Methodology

In this article, a new methodology [19] suggested by Weather Data Task Force, IEA EBC Annex 80 is used to generate future weather files and detect heatwaves in future periods for Copenhagen. The methodology is based on consecutive steps as represented in the flow Figure 1 below. The life cycle of most buildings is about 50-100 years, so we divide this century into three reference periods: historical (2001-2020), mid-term future (2041-2060) and long-term future (2081-2100). We generated Typical Meteorological Years (TMYs) and detected HWEs for Copenhagen for these three periods, based on the CORDEX climate data and the observed climate data in the reference historical period (2000-2019).

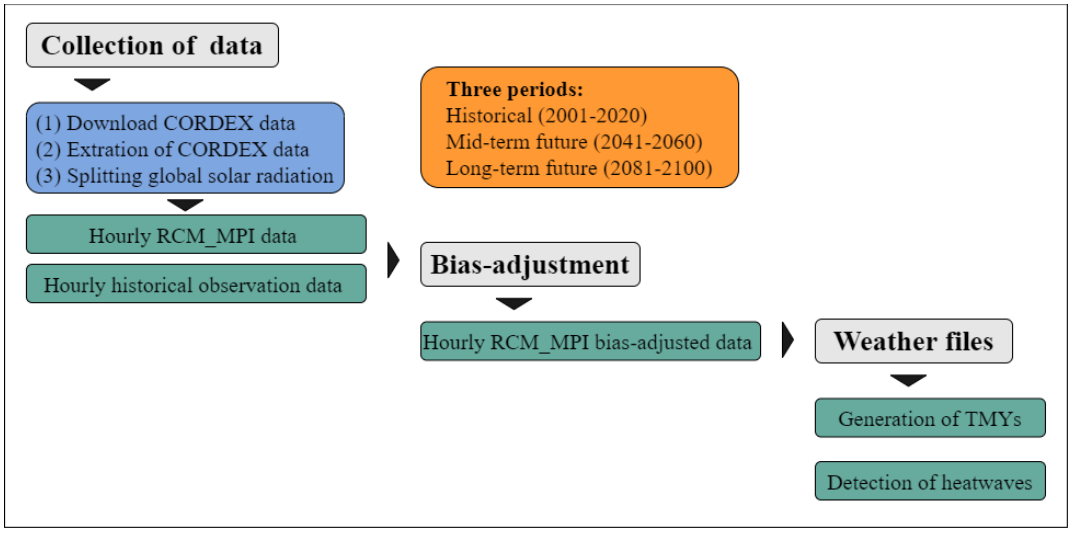

Figure 1. Flow of the generation of the weather data in Copenhagen (modified based on [20])

2.1 Collection and process of data

2.1.1 Climate model

Through more than 50 years of research, several different climate models have been developed and proposed for the prediction and generation of future meteorological data. The first climate was proposed by Norman Phillips in 1956 who developed a mathematical model that could realistically depict monthly and seasonal patterns in the troposphere [21]. Then the first Global climate model

(GCM) was created by NOAA's Geophysical Fluid Dynamics Laboratory and the model still stands today as a breakthrough of enormous importance for climate science and weather forecasting [22]. For the past two decades, the most widely used climate model is the GCMs which is driven by large-scale climate forcing such as the distribution of oceans and continents, the presence of large continental surfaces such as mountains, etc [19] [23]. With the development of climate models, the resolution of GCMs has increased from 500km in 1990 to 100km in 2007 (IPCC Fourth Assessment Report), but GCMs still has serious difficulties in reproducing daily precipitation and temperature [24]. To improve the simulation resolution, several downscaling models were derived based on the global climate models, including statistical and dynamical models. The statistical models such as Morphing [7] and Stochastic [25] use simple methods and low computational power, but the climate change is only represented through monthly averages and lack of physical consistency between weather variables. Beyond that, future extreme events are not represented on these methods.

Regional Climate Models (RCMs) which were essentially developed with the aim of downscaling climate fields (less than 100 km^2) [26] [27] produced by coarse resolution GCMs (150–600 km^2), thereby providing information at fine, sub-GCM grid scales are more suitable for studies of regional phenomena and application to vulnerability, impacts, and adaptation (VIA) assessments [27] (Figure 2). RCMs allow the representation of extreme events (in comparison with statistical downscaling), such as heatwaves and they also allow to consider model uncertainties (by comparing different model outputs) [28]. However, most of RCMs models such as the CORDEX platform, the data are not bias-adjusted [29] [30].

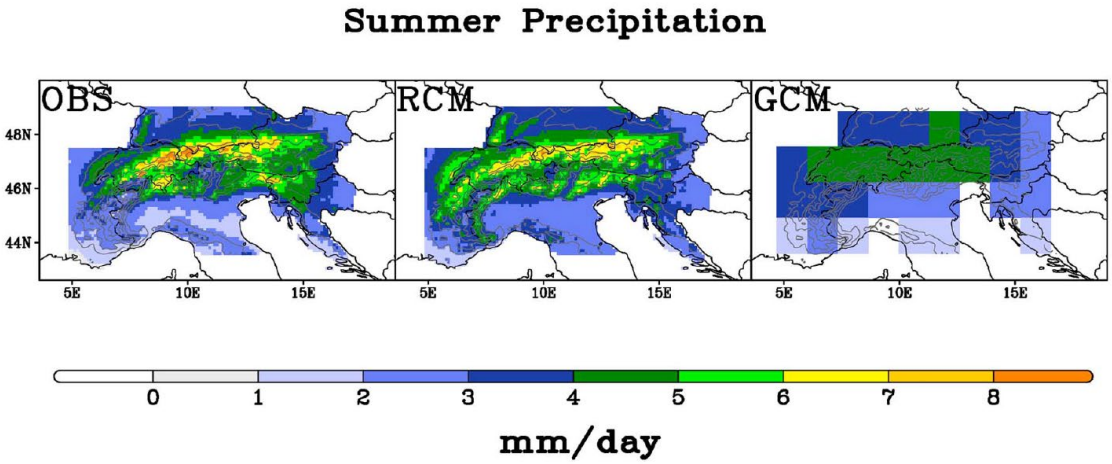

Figure 2. Simulation of summer precipitation over the Alpine region [27].(left) Observations ; (middle) RCM ensemble (~ 12-km grid spacing); (right) GCM ensemble (~ 150-km grid spacing). Units are in mm/day, and the simulation period is 1975–2004.. RCM = regional climate model; GCM = global climate model

2.1.2 . Climate scenarios and projections

For the future climate scenarios and projections, climate projections are typically presented for a range of plausible pathways, scenarios, or targets that capture the relationships between human choices, emissions, concentrations, and temperature change, as shown in Figure 3. Cumulative emissions of CO_2 largely determine global mean surface warming by the late 21st century and beyond [31].

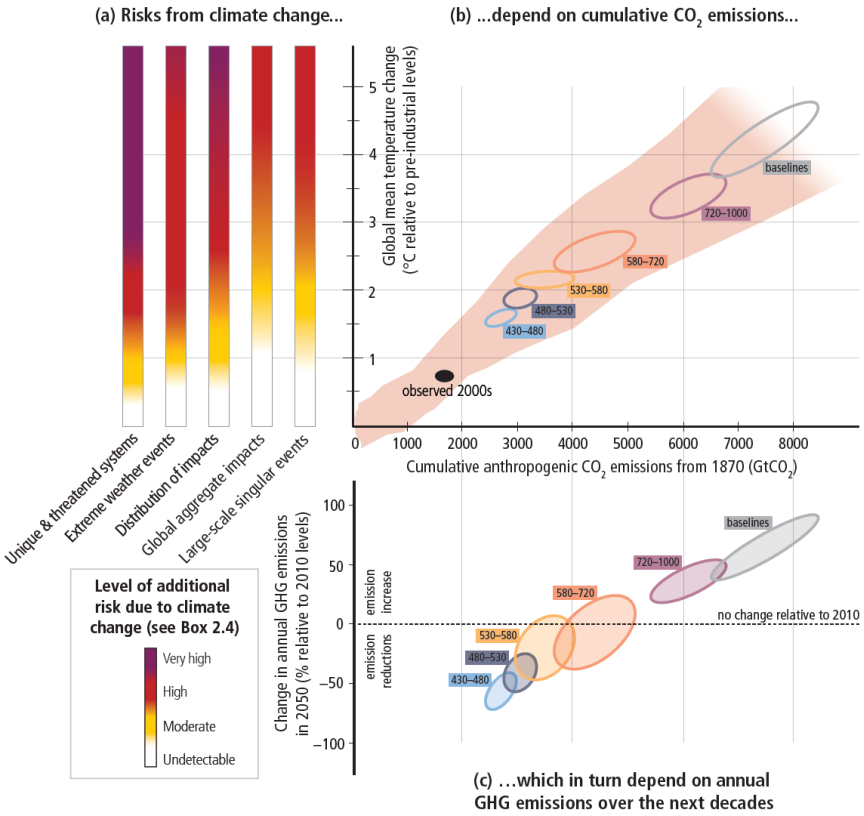

Figure 3. The relationship between risks from climate change, temperature change, cumulative carbon dioxide (CO2) emissions and changes in annual greenhouse gas (GHG) emissions by 2050. Limiting risks across Reasons for Concern (a) would imply a limit for cumulative emissions of CO2 (b), which would constrain annual emissions over the next few decades (c). Adapted from [31].

The first set of long-term emissions scenarios were developed by Intergovernmental Panel on Climate Change (IPCC) in 1990 and 1992 [32]. In 1995, the scenarios were evaluated and the evaluation recommended that significant changes (since 1992) in the understanding of driving forces of emissions and methodologies should be addressed. In 2000, the Special Report on Emissions Scenarios (SRES) was commissioned by the IPCC [33] and these scenarios have been used in the climate model simulations assessed in both the IPCC 2001 and 2007 reports. As SRES scenarios do not explicitly incorporate carbon emissions controls, in 2010, Representative Concentration Pathways (RCPs) were established, which are expressed in terms of greenhouse gas concentrations instead of emission levels [34].

In this work, to get the future weather data and the extreme weather conditions like heatwaves based on current emissions, a 'business-as-usual' approach (RCP8.5) with very high GHG emissions (RCP8.5) was used to describe the greenhouse gas concentrations in the future which means by 2100, the atmospheric concentrations of CO_2 are three to four times higher than pre-industrial levels and the global temperature will rise about 5°C [34][35], see Figure 4.

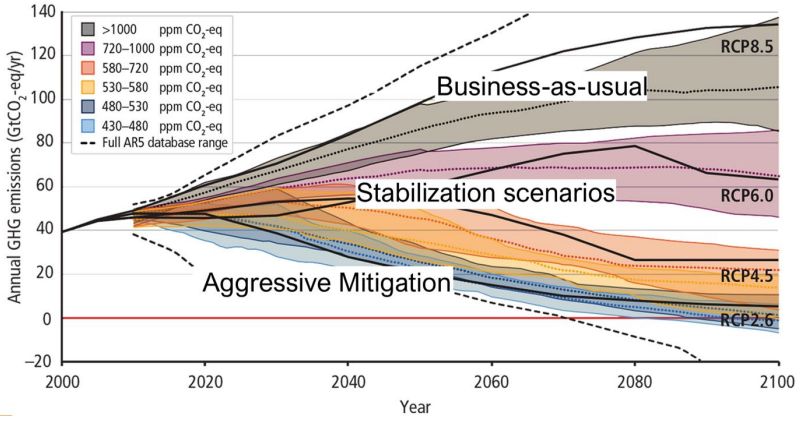

Figure 4. Representative Concentration Pathways; Adapted from [31]

2.2 EURO-CORDEX Climate data

Climate impact assessments and the development of regional to local-scale adaptation strategies require the availability of high-resolution climate change scenarios, including an assessment of their robustness and their inherent uncertainties [36]. A new high-resolution regional climate change ensemble has been established for Europe within the World Climate Research Program Coordinated Regional Downscaling Experiment (EURO-CORDEX) initiative that is a program sponsored by World Climate Research Program (WCRP) to develop an improved framework for generating regional-scale climate projections for impact assessment and adaptation studies worldwide within the IPCC AR5 timeline and beyond [37]. This includes harmonization of model evaluation activities in the individual modeling centers and the generation of multi-model ensembles of regional climate projections for the land-regions worldwide [38]. Two types of weather data are necessary to generate such weather datasets for Copenhagen, one of them is the Sub-daily Regional Climate Model (RCM) data projections from the CORDEX project, another is the historical hourly observations of relevant climate parameters. The CORDEX RCM climate simulation results are available from 1950 to 2100. This allows generating both typical meteorological years using representative time periods for historical, future mid-term and future long-term and to detect extreme events such as heatwaves in the future. Historical hourly observations are necessary to validate and correct climate projections through bias-correction techniques. We collected observation data from Copenhagen in the period of 2000-2019 from the local meteorological station, including hourly data of dry-bulb temperature, relative humidity, wind speed and global solar radiation.

2.3 Download and Extraction of CORDEX data

The downscaling method and driving model to be selected are reported in Table 1 below. In this report, only the "average" model MPI was considered which is well supported by the literature [26] [39] [40] [41]. For Copenhagen, Europe CORDEX hourly data have been downloaded including five parameters (Air Temperature, Relative Humidity, Wind Speed, Air Pressure, Global Solar Radiation) which are necessary climate variables to reconstruct a weather file for at least one future RCP scenario in three reference periods (2001-2020, 2041-2060, 2081-2100) in NetCDF format and the data was extracted in CSV format by using python code. It allows finding the closest data point on the grid to a given set of latitude and longitude [19]. The calculation of energy used in buildings and the performance of solar devices requires diffuse and direct solar radiation, which are not available in the MPI model, so we split them from the hourly values of global radiation through the solar radiation model [42] [43].

Table 1. The climate mode in COREDX data ([20])

Continent	Domain	Downscaling Method	Driving Model *	Time Frequency
Europe	EU-11	REMO 2015	MPI-M-MPI-ESM-LR	1 HOUR
Africa	AFR-22	REMO 2015	MPI-M-MPI-ESM-LR	3 HOURS
Asia	SEA-22	REMO 2015	MPI-M-MPI-ESM-LR	3 HOURS
South America	SAM-22	REMO 2015	MPI-M-MPI-ESM-LR	3 HOURS
North America	NAM-22	REMO 2015	MPI-M-MPI-ESM-LR	3 HOURS

2.4 Bias-Correction

There is a bias between climate model simulated data and observations because of many reasons like the coarse spatial resolution of climate model simulations, the inability to mathematically model climate processes and feedbacks, the limits in computational and time resources, continuously evolving climate sciences. Different degrees of biases in different variables may lead to unrealistic building responses, and inaccurate projected changes in building performance. The goal of bias correction is to reduce long-term bias associated with climate model data. Care is taken to ensure that projected changes in climate are preserved, and bias-corrected climate is physically consistent [44].

Here, a multivariate bias correction technique MBCn was used to perform bias correction by R [45], which is a modification of the N-pdft algorithm used in computer vision and image processing [46], is developed as a multivariate bias correction algorithm for climate model simulations of multiple variables. The result is a multivariate generalization of quantile mapping that transfers all statistical characteristics of an observed continuous multivariate distribution to the corresponding multivariate distribution of simulated variables. Unlike other multivariate bias correction algorithms [47] [48], MBCn is not restricted to correcting a specified measure of joint dependence, such as Pearson or Spearman rank correlation, nor does it make strong stationarity assumptions about climate model temporal sequencing. The underlying N-pdft algorithm also has proven convergence properties [46].

Firstly, MBCn applies random orthogonal rotations to model simulated and observed climate data, then perform univariate quantile delta mapping bias correction on the rotated climate data, thirdly, apply inverse rotation to corrected climate data to obtain multivariate ranking structure and finally, apply univariate quantile delta mapping and reorder variables considering multivariate ranking structure obtained in the third step [49] [50] [48]. The historical (2001-2019) observation data were used to correct the bias of the CORDEX climate data in the same period, and the future (2041-2060, 2081-2100) CORDEX data was corrected by historical data. The probability density function (PDFs) of the bias-correct CORDEX data are shown in Figure 5.

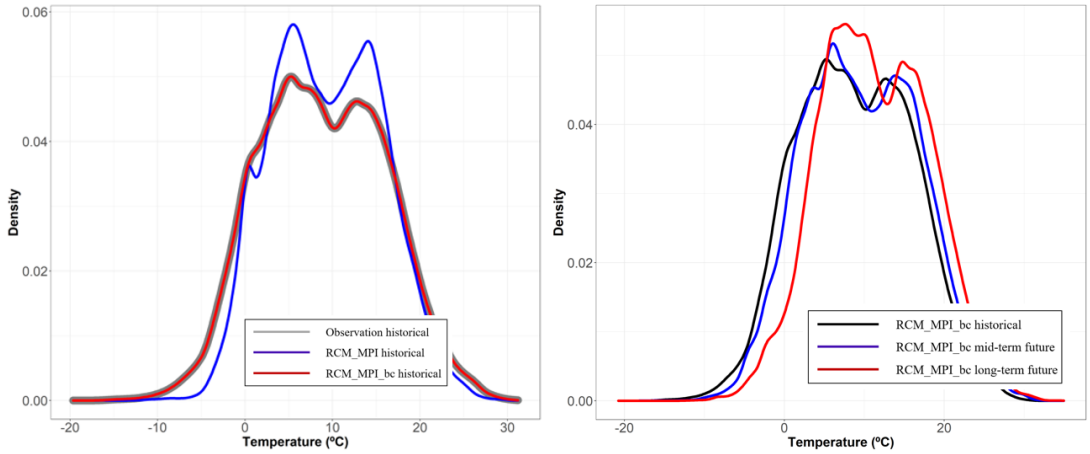

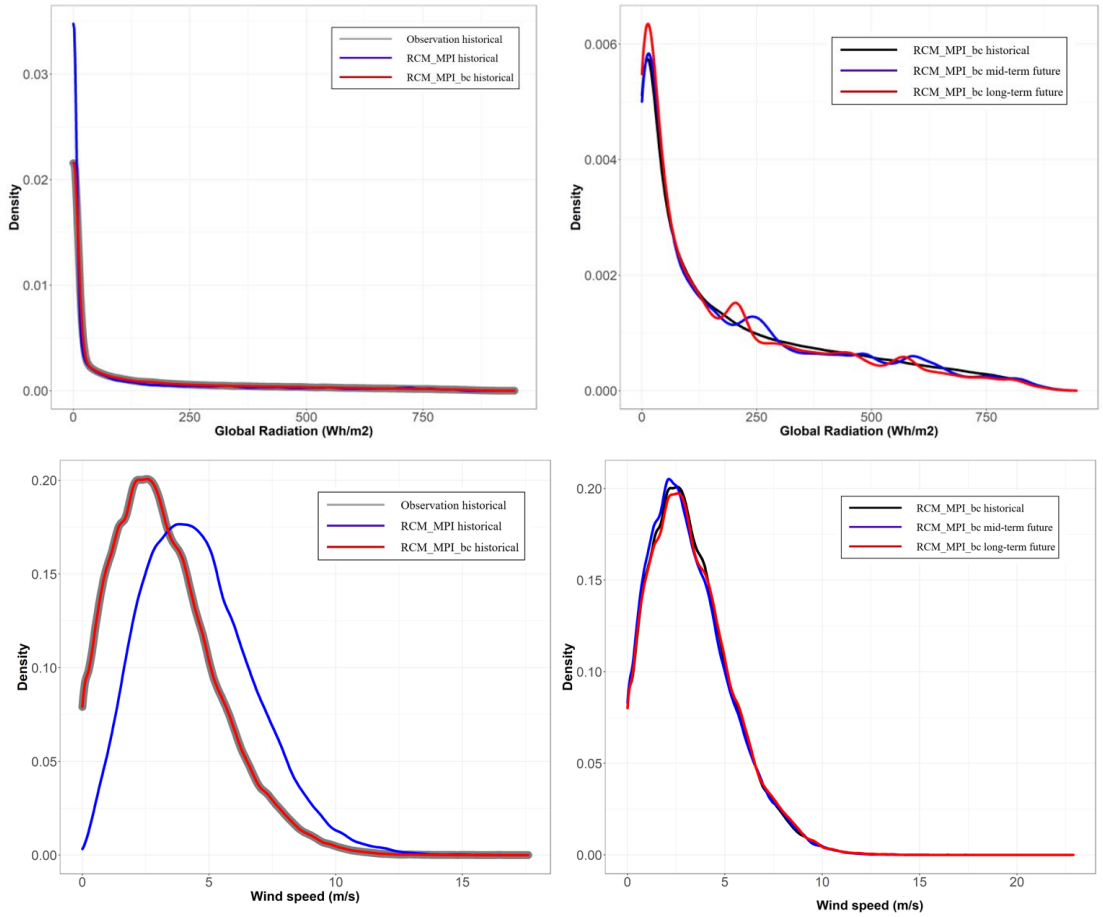

Figure 5. PDFs results for the bias-correction (RCM_MPI: RCM_MPI CORDEX climate data; RCM_MPI_bc: RCM_MPI CORDEX climate bias corrected data.)

2.5 Generation of future weather files

2.5.1 Typical Meteorological Years (TMY)

Typical Meteorological Years are commonly used for building simulations. The TMY methodology was introduced in 1978 and consists of the selection of twelve typical months from 30 years of hourly data to assemble one year of representative weather data for a given location [51] which of the twelve typical months were selected by statistical analysis of 9 different variables using different weighting factors used to rank the 30 months that are available for each month [52] [53]. There is no consistent method to produce a typical year. The main difference comes from the number of variables and their weight factors[4].

In this section, the methodology of the standard NF EN ISO 15927-4 was used to generate the TMY data [19] [54]. Four parameters were used to select the most typical months among the years: The dry-bulb temperature, the relative humidity, the global horizontal radiation of equivalent first order, and the wind speed of second order. TMY is constructed from '12' representative months (Best months) from multi-year records. The selection of 'Best months' is done by comparing the CDF of the single and reference years through the Finkelstein-Schafer (FS) statistics. For selecting the 'Best months', two sets of parameters (p) are taken into account, one of them is the primary parameters which including dry-bulb air temperature, global solar irradiance and relative humidity (or alternatively air absolute humidity, water vapor pressure or dew point temperature), and another one is the secondary parameter which is wind speed.

To get the 'Best months', the daily means calculated from 20 years of hourly values of each parameter firstly. For each year (y) of the data set, calculate the cumulative distribution function of

the daily means within each calendar month, F(p,y,m,i), by sorting all the values for that month and that year in increasing order and then using following equation , where J (i) is the rank order of the value of the daily means within that month and that year.

$$F(p,y,m,i) = \frac{J(\overline{p_i})}{n+1} \quad (1)$$

For each calendar month (m), calculate the cumulative distribution function of the daily means overall years in the data set, ϕ(p,m,i), by sorting all the values in increasing order and then using the following equation, where K(i) is the rank order of the value of the daily means within that calendar month in the whole data set.

$$\Phi(p,m,i) = \frac{K(\overline{p_i})}{N+1} \quad (2)$$

For each calendar month, calculate the Finkelstein –Schafer statistic, FS (p,y,m), for each year of the data set.

$$F_s(p,y,m) = \sum_{i=1}^{n} |F(p,y,m,i) - \Phi(p,m,i)| \quad (3)$$

For each parameter and for each calendar month, rank the individual months from the multiyear record in order of increasing size of FS (p,y,m). For each calendar month and for each year, add the separate ranks (R) for the three climate parameters.

$$R_{tot}(y.m) = R(T,y,m) + R(I,y,m) + R(WVP,y,m) \quad (4)$$

For each calendar month, for the three months with the lowest total ranking Rtot(y,m), calculate the deviation of the monthly mean wind speed from the corresponding multi-year calendar-month mean. The month with the lowest deviation in wind speed is selected as the “best” month to be included in the reference year.

2.5.2 Detection and characterization of future heatwave event (HWE)

In a future warmer climate with increased mean temperatures, it seems that heatwaves would become more intense, longer lasting, and more frequent, which associated with particularly hot sustained temperatures have been known to produce notable impacts on human mortality, regional economies, and ecosystems [55] [56]. It can be seen from the series of reported heatwave events that severe hot temperatures contributed to human mortality and caused widespread economic impacts, inconvenience, and discomfort [57]. In Denmark, a national heatwave is defined as a period of at least 3 consecutive days of which the maximum temperature across more than fifty percent of the country exceeds 28°C. The Danish Meteorological Institute further defines a “warmth wave” when the same criteria are met for a 25°C temperature limit.

In this report, a new method proposed by G. Ouzeau et al. [58] was used to detect heatwave event which was adapted to a EURO-CORDEX dataset. Unlike most of the previous definitions, which use absolute thresholds, three redefined thresholds as percentiles of daily mean temperature distribution over the historical period are defined to make the method accessible to any dataset as shown in Figure 6. S_{pic} represents the 99,5% threshold of the temperature distribution during the historical period and it is used to detect a heatwave. S_{deb} represents the 97.5% threshold of the temperature distribution during the historical period and it defines the heatwave duration. S_{int} represents the 95% threshold of the temperature distribution during the historical period and it determines the end of the heatwave if the temperature drops below. Three criteria were characterized by this method for every heatwave: maximal temperature, duration and global intensity as shown in Figure 6. Heatwaves in Copenhagen were detected in three periods: the historical period (2001-2020), the mid-term future period (2041-2060) and the long-term future period (2081-2100). The temperature dataset in the historical period was used to define the three thresholds.

For the new HWE definition, the temperature thresholds were not considered to vary over time. It means that no thermal adaptation is envisaged, but the fact is that the thresholds may increase since the increase in temperatures will be offset by the adaptation of the population to heat [59]. To consider the impact of the adaptation of heat, many studies have been inspired by the work of Heat-Health Warning Systems [60][61]. The reference values for thresholds are determined from epidemiological studies which link heat to mortality data, i.e., by modeling the temperature-mortality relationship, which found the percentile of thresholds are constant in different periods [59]. It means that the improvement of people's thermal adaptability with global warming also needs to be considered when detecting the HWEs. In this study, we proposed a revised definition that detected HWEs by thresholds from the same percentile but based on the examined period. For example, the three temperature thresholds for the 2090s (2081-2100) with thermal adaptation HWEs were calculated by the 99.5%, 97.5%, 95% of the daily mean bias-adjusted COREX temperatures in 2090s not 2010s. Results and comparisons of four HWEs definitions are shown in section 3.2.

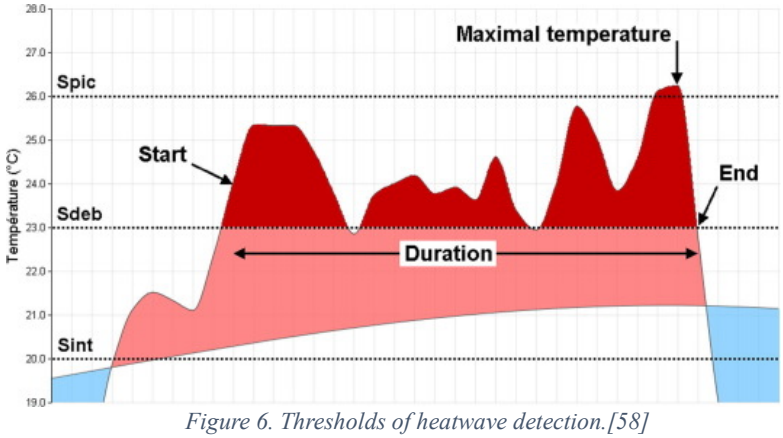

Figure 6. Thresholds of heatwave detection.[58]

3. Results and Discussion

3.1 Typical weather year data

In this section, we generated typical weather year data files for the three periods by re-assembling the selected typical months including dry-bulb temperature, solar radiation, relative humidity, wind speed and wind direction, and we also generated TMY data for historical observation data using the same method. These files were hourly data in EPW format and can be used as weather data on software like Energy Plus for the building simulation. In order to verify the quality of the dataset, we compared dry-bulb temperatures bias-adjusted from the RCM_MPI climate model and the ones generated by Meteonorm software which uses the detailed model for urban effects based on the H2020 climate-fit.city project [62]. The distribution of the hourly temperature data over the historical period (2010s), mid-future period (2050s) and long-term period (2090s) in TMY files are shown in Figure 7 and Figure 8. For the historical and mid-future periods, the temperatures between the two climates model are very close. For the long-term period, the temperatures from RCM_MPI are close to the Meteomorn until 15ºC, but for higher temperatures, the difference increase and the Meteomorn temperatures are finally higher about 4ºC. It can be seen from Table 2 that at 50% of the distribution, the temperatures in three periods are about 8.8ºC, 9.7ºC and 11.0ºC for MPI, and 8.6ºC, 9.9ºC and 11.0ºC for Meteonorm, and at 95% of the distribution, the temperatures in three periods are about 23.9ºC, 25.7ºC and 25.1ºC for MPI, and 25.7ºC, 25.6ºC and 29.7ºC for Meteonorm. The temperatures from Meteonorm are higher than that

from MPI for most of the time in all three period. At the end of the distribution for all models, the temperatures are very close.

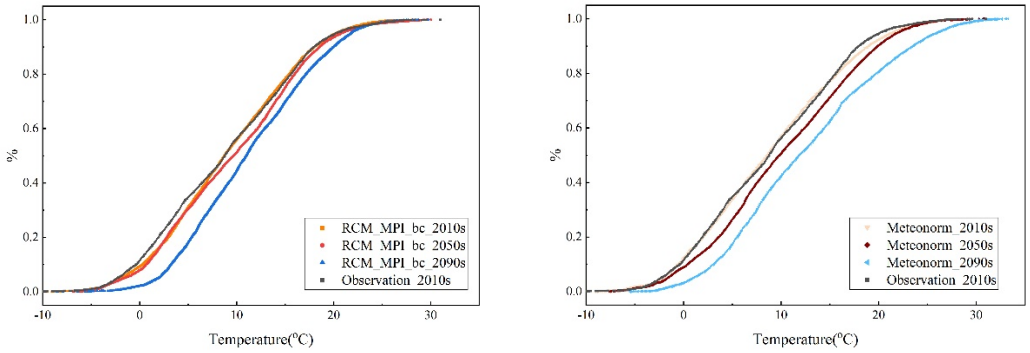

(a) (b)

Figure 7. Distribution of temperature in TMY datasets generated by different methods (a) RCM-MPI model (b) Meteonorm

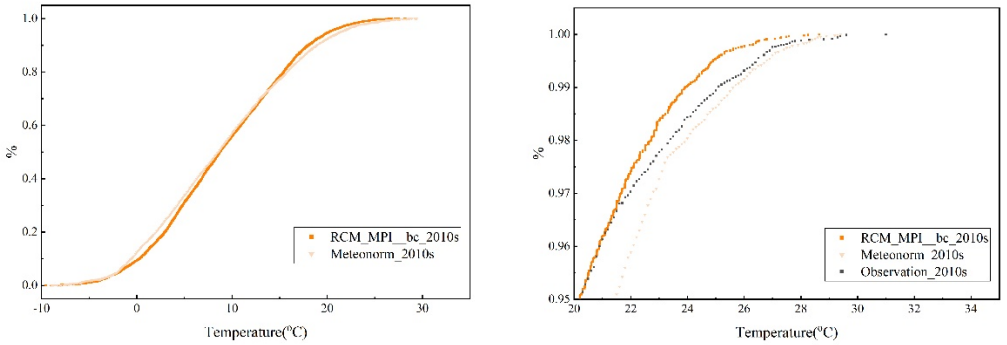

(a) (b)

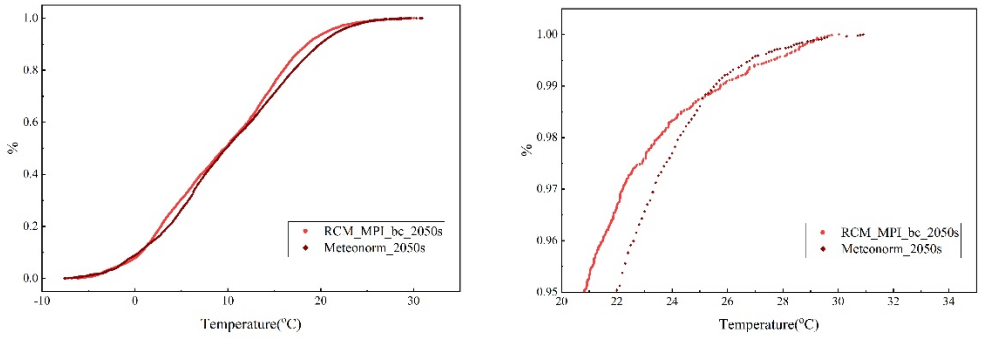

(c) (d)

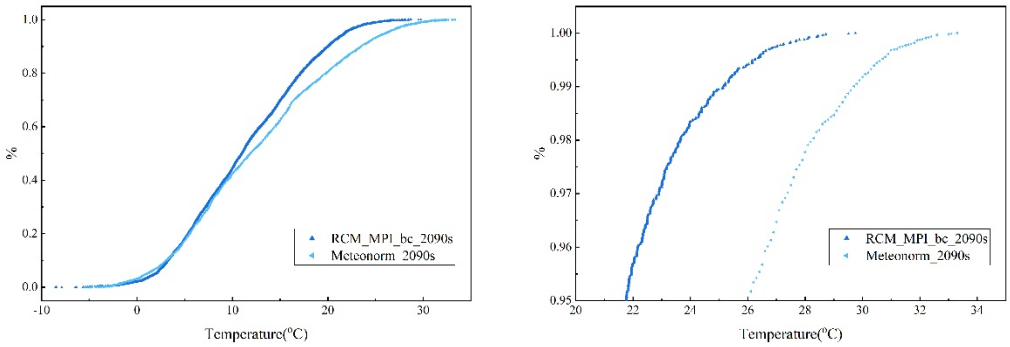

(e) (f)

Figure 8. Comparison of temperature predictions in three periods (a), (b) historical period (2010s), (c),(d) mid-future period (2050s), (e),(f) long-term period (2090s) Right: all data points, Left: over the 0.95 to 1 centile.

Table 2. 0.5, 0.95, 0.99 centiles of the temperature distribution between the three periods TMY.

Model/Periods		0.5		0.95		0.99	
		Hours(h)	Temp(°C)	Hours(h)	Temp(°C)	Hours(h)	Temp(°C)
Observation	2010s	4446	8.9	8322	20.2	8674	25.1
RCM-MPI	2010s	4380	8.8	8322	20.2	8673	23.9
	2050s	4380	9.7	8322	21.0	8673	25.7
	2090s	4380	11.0	8322	21.8	8673	25.1
Meteonorm	2010s	4395	8.6	8330	21.5	8677	25.7
	2050s	4400	9.9	8325	22.0	8676	25.6
	2090s	4396	11.9	8337	26.1	8673	29.7

To compare more clearly TMY results of different climate models in predicting high temperature, we need to analyze the results of summer separately because the impact of changes in the distribution of weather elements is different [63]. The hourly TMY temperature distributions during the summer in Copenhagen (June-August) are presented in Figure 9 and Figure 10. It can be seen that the difference in temperature distribution between the two climate models increases slightly in summer. During the historical period, the typical year summer hourly temperatures in Copenhagen protected by the model RCM_MPI with the new method for TMY are lower than the observations with the same TMY method. It can be explained by the fact that in Figure 5 since the bias-adjusted RCM_MPI data temperatures are lower than the observations. For the 0.5 and 0.95 distribution, as shown in Table 3, the temperatures are very close for the historical period, and the mid-term future period and that of Meteonorm are slightly higher than the RCM_MPI. For the end of the distribution tail (0.99), the observed temperature in the historical period is about 27.0°C and that of RCM_MPI model with the new TMY method is about 25.8 °C and that of Meteonorm with TMY3 method is about 27.5 °C. The difference between the two models in maximum temperature prediction will become more obvious in the long-term future which are 27.1°C and 31.4°C respectively.

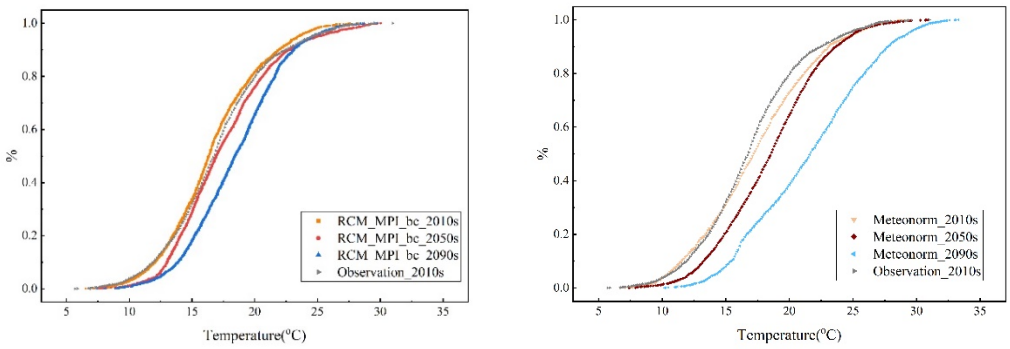

(a) (b)

Figure 9. Distribution of temperature in TMY datasets generated by different methods in Summer (June-August) (a) RCM-MPI model (b) Meteonorm

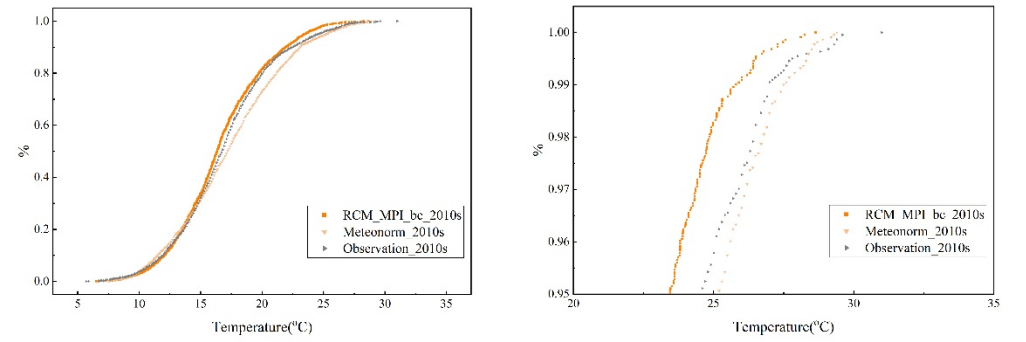

(a) (b)

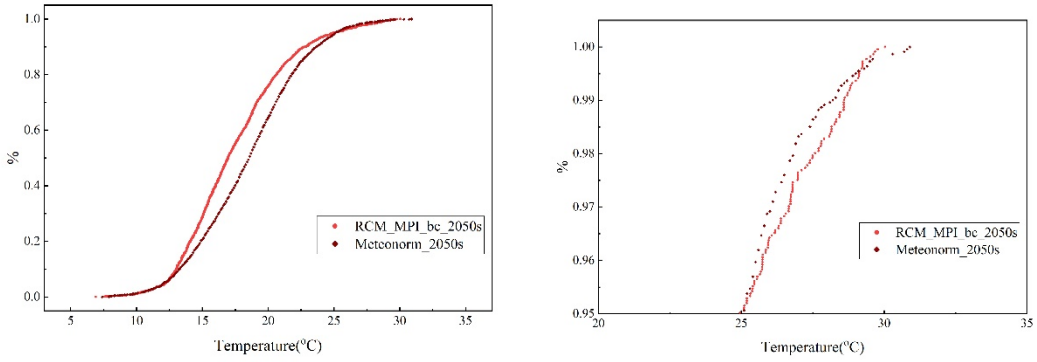

(c) (d)

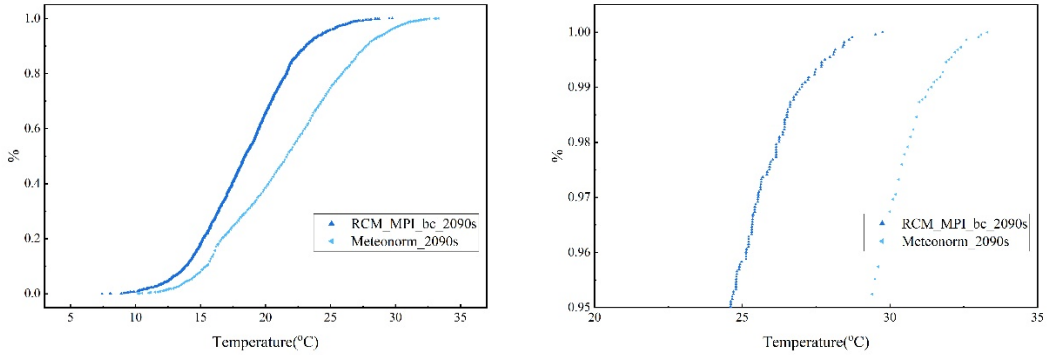

(e) (f)

Figure 10. Comparison of temperature predictions in summer (June-August) in three periods (a), (b) historical period (2010s), (c),(d) mid-future period (2050s), (e),(f) long-term period (2090s). Right: all data points, Left: over the 0.95 to 1 centile.

Table 3. Temperature increase for the two climate models for the 0.5, 0.95, 0.99 centiles of the temperature distribution between the three periods TMY summer (June-August).

Model/Periods		0.5		0.95		0.99	
		Hours(h)	Temp(°C)	Hours(h)	Temp(°C)	Hours(h)	Temp(°C)
Observation	2010s	4719	16.8	5720	24.6	5806	27.0
RCM-MPI	2010s	4728	16.4	5722	23.4	5810	25.8
	2050s	4728	16.9	5722	24.9	5810	28.6
	2090s	4728	18.4	5722	24.6	5810	27.1
Meteonorm	2010s	4712	17.2	5717	25.2	5808	27.5
	2050s	4716	18.6	5711	25.1	5809	28.3
	2090s	4723	21.7	5720	29.3	5810	31.4

We also compared solar radiation predictions bias-adjusted data, the average hourly value of global radiation, direct radiation and diffuse radiation for 24 hours from two different climate models are shown in Figure 11. It seems that the RCM-MPI climate model predicts lower global horizontal irradiance in the future compared with Meteonorm. In Meteonorm, the global irradiances are similar in all three periods.

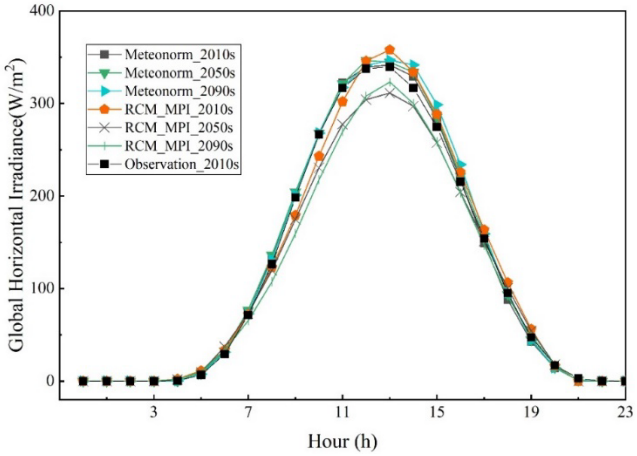

(a) Hourly mean global horizontal irradiance

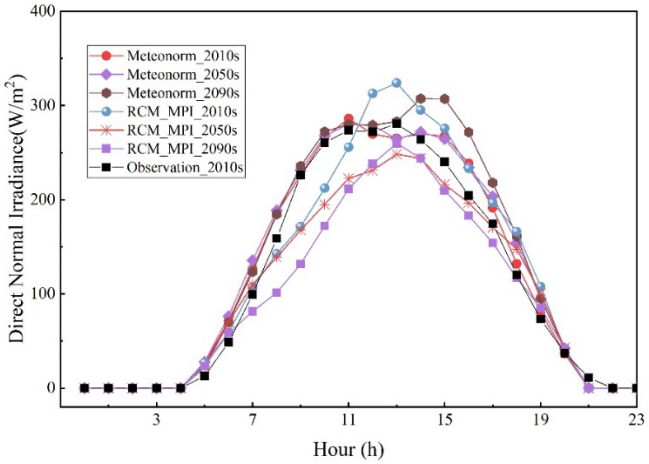

(b) Hourly mean direct normal irradiance

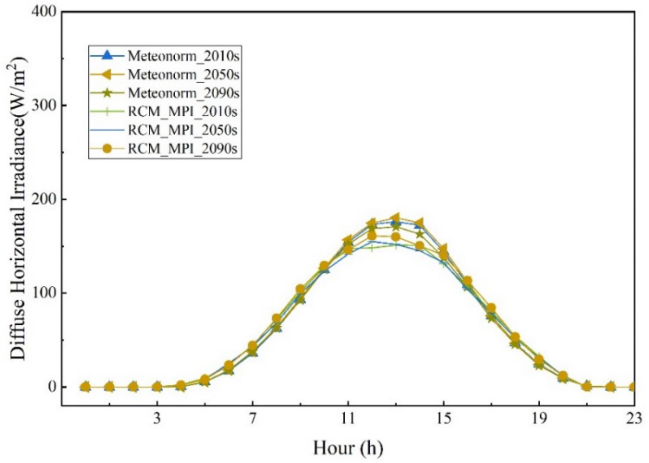

(c) Hourly mean diffuse horizontal irradiance

Figure 11. Comparison of the solar radiation of TMY data.

3.2 Heatwave detection

3.2.1 Estimated HWE without consideration of thermal adaptation

Following the approach described in the previous section, the three thresholds were obtained to define heatwaves as shown in Table 4 from the 20 years Copenhagen historical period (2010s). The three thresholds were 22.4ºC, 22.0ºC and 18.7ºC respectively. Bubble charts [58] illustrate the detected heatwaves in the history (2001-2020), mid-term future (2041-2060) and long-term future (2081-2100) periods, as shown in Figure 12. Each bubble represents a heatwave. The size of each bubble is characterized by its intensity in ºC. The intensity is the sum for each heatwave day of the positive difference between the daily mean temperature and the threshold S_{deb}, divided by the difference between the S_{pic} and S_{deb} thresholds. As shown in Table 6, the number of HWEs in 2050s and 2090s are 1.8 times and 2.5 times of that in 2010s respectively, and the duration of HWEs in 2050s and 2090s are on average 1.8 and 2.7 times of that in 2010s respectively, and the maximum daily mean temperature of HWEs in 2050s and 2090s are increase by 1.2ºC and 2.5ºC than that in 2010s respectively (Table 4). It can be seen that the heatwave events (HWEs) will be more frequent and severe in the long-term future period than the historical period no matter from which one characterization and the heatwave in mid-term future period is of similar maximum daily mean temperature but longer and more severe than the historical period.

Table 4. Thresholds; Duration; Maximum daily mean temperature. Without thermal adaptation. Periods 2001-2020; 2041-2060; 2081-2100.

Criteria	Periods Thresholds (°C)	2010s	2050s	2090s
Thresholds (°C)	S_{pic} (99.5)		22.4	
	S_{deb} (99)		20.0	
	S_{int} (95)		18.7	
Duration (Days)	Maximum	8.4	12.5	17.6
	Average	20.0	37.0	53.0
Maximum daily Mean Temperature (°C)	Maximum	23.4	24.1	24.2
	Average	25.1	26.3	28.6

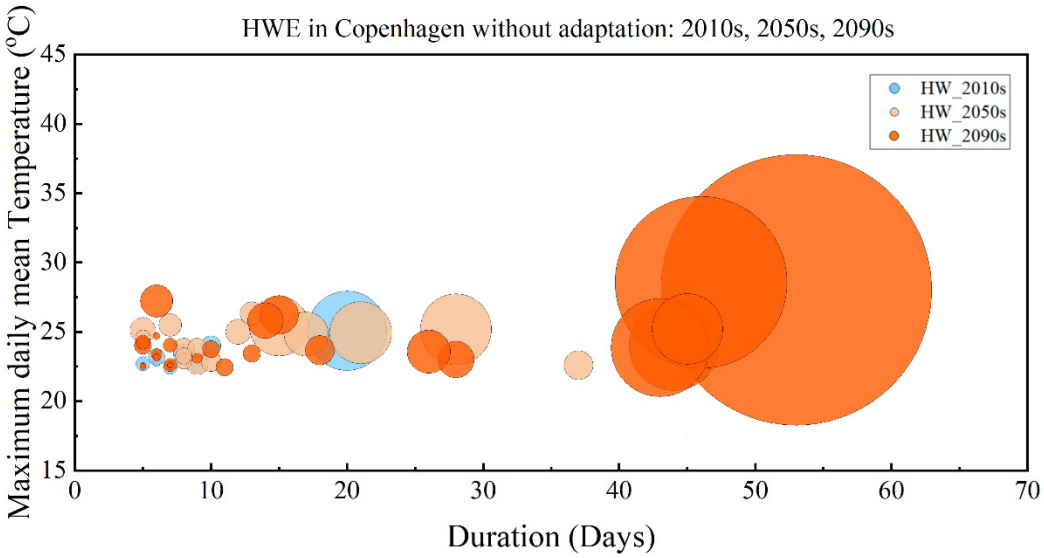

Figure 12. HWEs detected in Copenhagen without considering thermal adaptation during the three periods

3.2.2 Estimated HWE with consideration of thermal adaptation

In the new HWE definition the temperature thresholds were not considered to vary over time. It means that no thermal adaptation as envisaged, but the fact is that the thresholds may increase since the increase in temperatures will be offset by the adaptation of the population to heat [59]. To consider the impact of the adaptation of heat, many studies have been inspired by the work of Heat-Health Warning Systems [60][61]. The reference values for thresholds are determined from epidemiological studies which link heat to mortality data, i.e., by modeling the temperature-mortality relationship, which found the percentile of thresholds are constant in different periods [59]. It means that the improvement of people's thermal adaptability with global warming also needs to be considered when detecting the HWEs. In this work, we proposed a revised definition that detected HWEs by thresholds from same percentile but not based on historical period. For example, the three temperature thresholds for 2090s (2081-2100) with thermal adaptation HWEs were calculated by the 99.5%, 97.5%, 95% of the daily mean bias-adjusted COREX temperatures in 2090s not 2010s. The thresholds for HWEs with adaptation in 2050s and 2090s were 1.2°C and 2.3°C warmer than that of without adaptation, respectively (Table 5). During the same periods, the average temperature in summer (June to August) was 1.0°C and 2.0°C higher than that of 2010s. The HWEs detected in three periods by the definition with adaptation were shown in Figure 13. It can be seen that the size and the number of the bubbles for periods of 2050s and 2090s will decrease a lot compares to the HWEs without adaptation, because of the higher temperature thresholds. In contrast to the HWEs without adaptation, the number of HWEs with adaptation in the

future will be fewer and fewer, from 10 times per year in 2010s to 5 times per year in 2090s (Table 6). The maximum daily mean temperature in 2090s was 3.5°C warmer than that of 2010s, while the average air temperature rose by 2.3°C during the same periods. It suggests that overall temperature increases will be more pronounced in the future than extreme temperature and the thermal adaptation is important to be considered, when defining future HWE.

Table 5. Thresholds; Duration; Maximum daily mean temperature. With thermal adaptation. Periods 2041-2060; 2081-2100.

Criteria	Periods Thresholds (°C)	2010s	2050s	2090s
Thresholds (°C)	S_{pic} (99.5)	22.4	23.6	24.7
	S_{deb} (99)	20.0	21.2	22.2
	S_{int} (95)	18.7	19.9	21.0
Duration (Days)	Maximum	8.4	10.4	15.0
	Average	20.0	16.0	38.0
Maximum daily Mean Temperature (°C)	Maximum	23.4	25.1	27.2
	Average	25.1	26.3	28.6

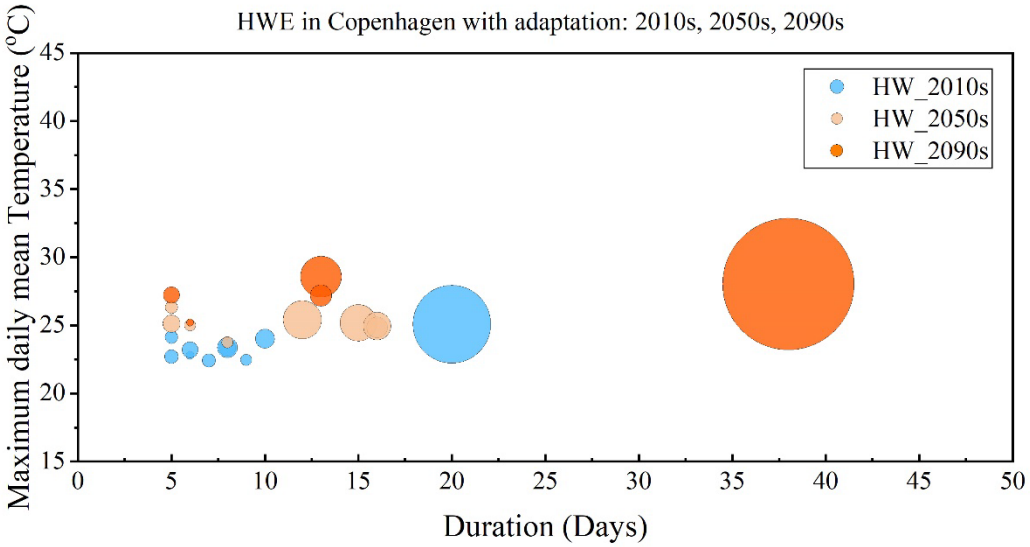

Figure 13. Heatwaves detected in Copenhagen considering thermal adaptation during the three periods.

3.2.3 HWEs definition in Denmark

Regardless of whether thermal adaptation was considered or not, the above methods were based on daily mean temperature to obtained temperature thresholds of HWEs. In Denmark, the Danish Meteorological Institution (DMI) use three consecutive days of maximum daily temperature to define two types of HWEs, which include 25°C for warm HWEs and 28°C for hot HWEs. It can be seen in Table 6 that the number of HWEs detected by the new definition without adaptation was slightly more than that of the DMI hot definition, and the DMI warm definition got the largest number of HWEs which was 4-10 times more than that of with adaptation depends on the different period.

Table 6. Number of HWEs for Four definitions.

Periods	2010s			2050s				2090s			
Definition	without/ with	DMI-Warm	DMI-Hot	without	with	DMI-Warm	DMI-Hot	without	with	DMI-Warm	DMI-Hot
Number of HWEs	10	42	4	18	8	38	18	25	5	56	16

The duration and the maximum temperature of the HWEs are the most significant factors of building overheating and thermal comfort in extreme climate conditions.. The Longest HWE for the four definitions were compared for each period as shown in Figure 14. It is apparent that the duration of heatwaves will increase in the future, regardless of which definition was used to detect HWE, except for the DMI_hot definition, whose duration of HWEs was about 15 days for all periods. For the new HWE definition without adaptation, the duration of the longest HWE was from about 20 days in 2010s to about 50 days in 2090s. For the longest HWE detected by the without adaptation definition in 2050s, at least 1/3 of the time when the daily maximum temperatures were below the DMI_warm threshold (25oC). The duration of the longest HWE of new definition with adaptation was between that of DMI_warm and DMI_hot, which was from about 20 days in 2010s to about 37 days in 2090s.

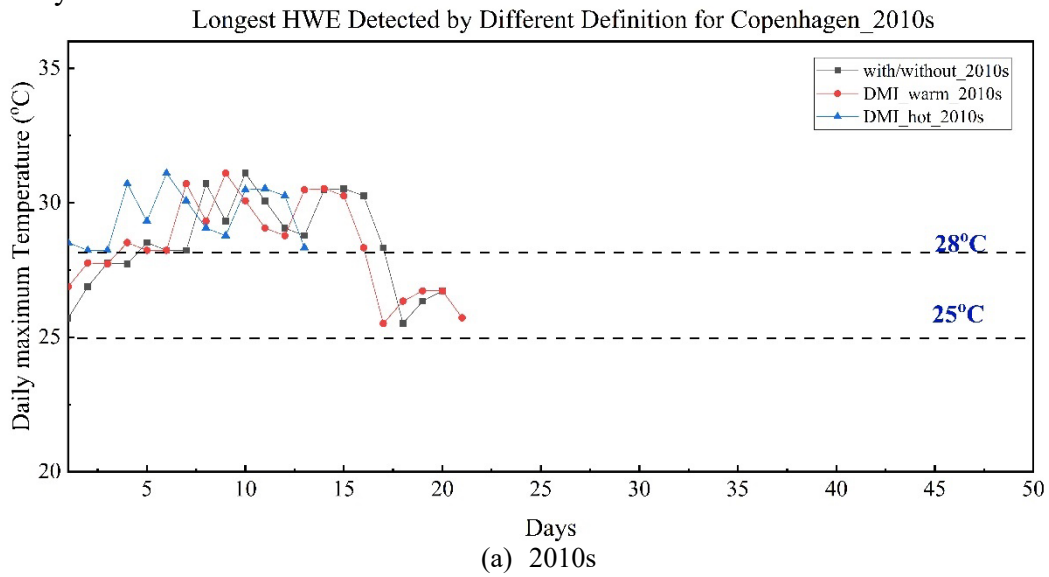

(a) 2010s

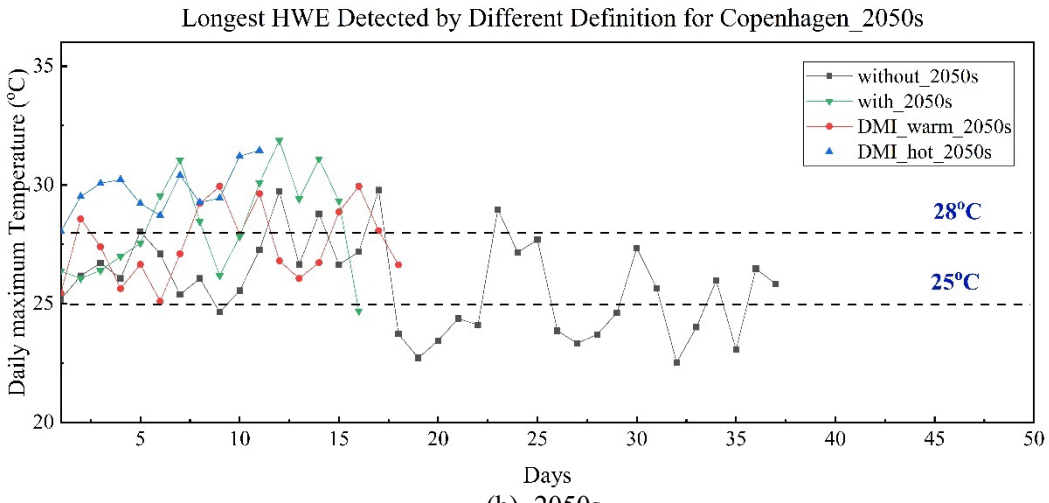

(b) 2050s

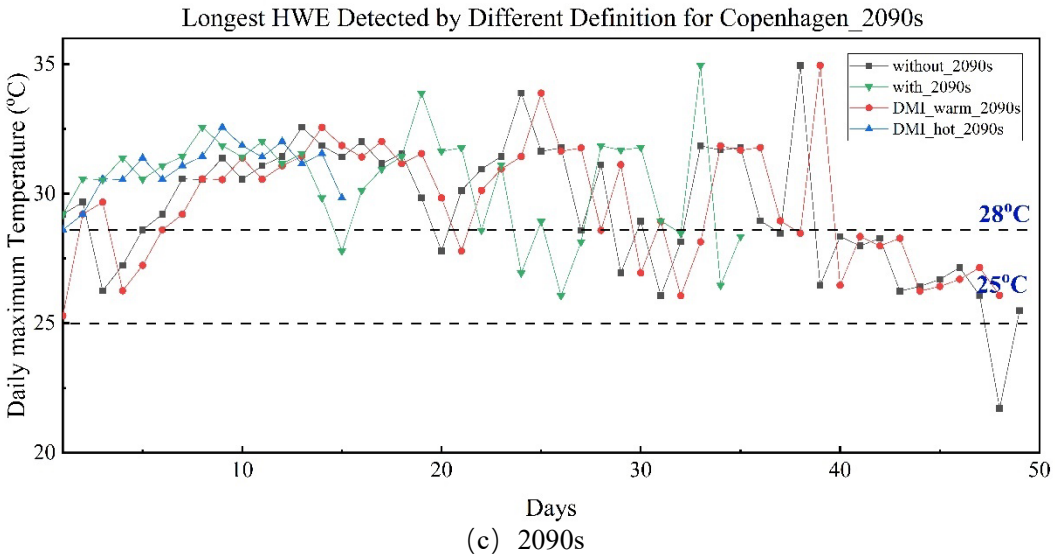

Figure 14. Longest HWE for four definitions: new definition with/without thermal adaptation, DMI warm/hot

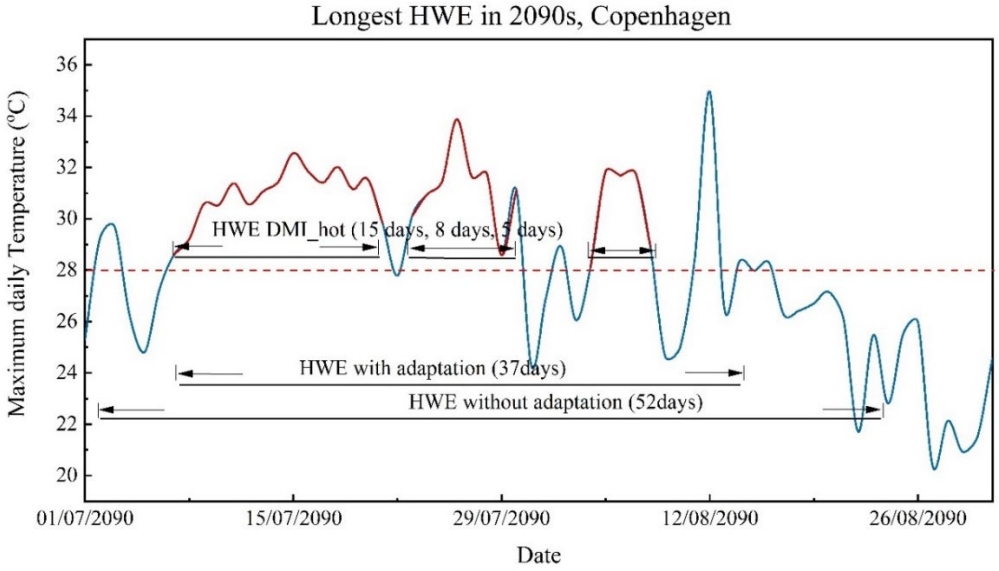

Figure 15. Maximum daily temperature during the most severe heatwave period.

In general, the definition of DMI_hot has the higher temperature thresholds than other definitions which recorded over month-long HWE in 2090s. But it was contradictory that the DMI_hot detected more HWEs than the new definition with adaptation (Table 6). Figure 14 plotted the daily maximum temperature in 2090 summer when the longest HWE was detected during the long-term period (2081-2100). It was found that three HWEs were detected by DMI_hot definition which were 15 days, 8days and 5days respectively, within the 37 days which was detected by the new definition with adaptation. The main reason is that the mean temperature will increase a lot due to climate change. Therefore, when determining the temperature thresholds of heatwave, taking the mean temperature into account becomes essential in the definition of heatwave. A relatively complete and independent HWE is the ideal research object, when studying the influence of the appearance and disappearance of heatwave on building overheating and building cooling load. Therefore, for the three HWEs highlighted in red in Figure 15, they can be considered as one long-time HWE. The average temperature as a threshold may reflect a continuous period of extreme weather better than the maximum temperature.

4. Conclusions

In this study, we introduced a new method suggested by Weather Data Task Force, IEA EBC Annex 80 which can generate future typical meteorological years and detect future HWEs by using the climate multi-year data from the EURO-CORDEX project. We used this method to generate weather datasets including dry-bulb temperature, relative humidity, solar radiation and wind speed in historical, mid-term future and long-term future periods for Copenhagen. Observation weather data in the historical period was used for bias-correction. We compared the TMY weather data files generated by the new method with those generated by Meteonorm. The TMY data of temperature and radiation generated by the new method agrees well with both the observation data and the Meteronorm data in the historical period. The TMY data of temperature from Meteonorm are always higher than the temperatures generated by new method for the same distribution in the future periods, because not only temperature but also other the three parameters were used to select the typical month for the new method. It is necessary to notice that in the long-term future, the temperature in Copenhagen will increase by 2oC-4oC, which poses challenges to cooling load and performance of buildings in the future.

For extreme weather conditions like heatwaves, it cannot be described by TMY files alone. How to define and characterize heatwaves are very interesting to study. A new definition suggested by IEA EBC Annex 80 was used to detect HWEs in three time periods in Copenhagen. The method does not consider thermal adaptation to weather changes. It shows that the HWEs will be more frequent and severe in the long-term future period than in the historical period no matter the characterization of the heatwave, and in the mid-term future period the HWEs are of similar maxima, but longer and more severe than in the historical period. Considering the thermal adaptability to increased temperatures in the future, we detected HWEs by thresholds from the same percentile but based on the actual period. The thresholds for HWEs in 2050s and 2090s were 1.2oC and 2.3oC higher than that of the historical period, and the average temperature in summer (June to August) was 1.0oC and 2.0oC higher than that of 2010s during the same periods. Under the assumption of thermal adaptation, the duration of future heatwaves will still significantly increase, but the frequency will not increase or even decrease. The maximum daily mean temperature is increased by 3.5oC from 2010s to 2090s, and at least 2.3oC of the increase is due to an increase in the average temperature. It suggests that the overall temperature increases will be more pronounced in the future than the extreme temperatures. The temperature thresholds of the above definitions were based on daily mean temperature, while the HWEs definitions of Danish Meteorological Institution were based on daily maximum temperature. It can be seen that the temperature threshold for DMI_hot definition was higher than other definitions which recorded over month-long HWE in 2090s, but in fact, it is very close to the HWEs detected considering thermal adaptation in 2090s for Copenhagen if we regard the HWEs occurring in succession over a period of time as one HWE. In conclusion, HWEs detected by the temperature thresholds calculated by the daily mean temperature are more independent and complete than that detected by the temperature thresholds calculated by the daily maximum temperature. It can be more conducive to the study of the impact of the heatwave on the indoor thermal environment and cooling load of buildings during and after the heatwave. Based on the current level of adaptation to heat, heatwaves in Copenhagen will be more frequent and longer in the future. However, it may not become more frequent if the adaptation to temperature changes is considered even though it will still become longer.

Reference

[1] O. Mazdiyasni and A. AghaKouchak, 'Substantial increase in concurrent droughts and heatwaves in the United States, *Proc. Natl. Acad. Sci.*, vol. 112, no. 37, pp. 11484–11489, Sep. 2015, doi: 10.1073/pnas.1422945112.

[2] R. S. Kovats and L. E. Kristie, 'Heatwaves and public health in Europe', *Eur. J. Public Health*, vol. 16, no. 6, pp. 592–599, Dec. 2006, doi: 10.1093/eurpub/ckl049.

[3] M. Stefanon, F. D'Andrea, and P. Drobinski, 'Heatwave classification over Europe and the Mediterranean region', *Environ. Res. Lett.*, vol. 7, no. 1, p. 014023, Mar. 2012, doi: 10.1088/1748-9326/7/1/014023.

[4] M. Herrera *et al.*, 'A review of current and future weather data for building simulation', *Build. Serv. Eng. Res. Technol.*, vol. 38, no. 5, pp. 602–627, Sep. 2017, doi: 10.1177/0143624417705937.

[5] E. Kjellström *et al.*, 'European climate change at global mean temperature increases of 1.5 and 2 °C above pre-industrial conditions as simulated by the EURO-CORDEX regional climate models', *Earth Syst. Dyn.*, vol. 9, no. 2, pp. 459–478, May 2018, doi: 10.5194/esd-9-459-2018.

[6] J. Bravo Dias, G. Carrilho da Graça, and P. M. M. Soares, 'Comparison of methodologies for generation of future weather data for building thermal energy simulation', *Energy Build.*, vol. 206, p. 109556, Jan. 2020, doi: 10.1016/j.enbuild.2019.109556.

[7] S. Belcher, J. Hacker, and D. Powell, 'Constructing design weather data for future climates', *Build. Serv. Eng. Res. Technol.*, vol. 26, no. 1, pp. 49–61, Feb. 2005, doi: 10.1191/0143624405bt112oa.

[8] V. Weilnhammer *et al.*, 'Extreme weather events in europe and their health consequences – A systematic review', *Int. J. Hyg. Environ. Health*, vol. 233, p. 113688, Apr. 2021, doi: 10.1016/j.ijheh.2021.113688.

[9] A. De Bono, P. Peduzzi, S. Kluser, and G. Giuliani, 'Impacts of Summer 2003 Heat Wave in Europe', 2004, Accessed: Oct. 18, 2021. [Online]. Available: https://archive-ouverte.unige.ch/unige:32255

[10] M. Santamouris, 'Cooling the buildings – past, present and future', *Energy Build.*, vol. 128, pp. 617–638, Sep. 2016, doi: 10.1016/j.enbuild.2016.07.034.

[11] L. Grignon-Massé, P. Rivière, and J. Adnot, 'Strategies for reducing the environmental impacts of room air conditioners in Europe', *Energy Policy*, vol. 39, no. 4, pp. 2152–2164, Apr. 2011, doi: 10.1016/j.enpol.2011.02.004.

[12] J. Hacker, S. E. Belcher, and A. White, 'Design Summer Years for London', May 2014.

[13] 'heat wave | meteorology | Britannica'. https://www.britannica.com/science/heat-wave-meteorology (accessed Nov. 16, 2021).

[14] 'Extreme Heat Services for South Australia'. http://www.bom.gov.au/announcements/media_releases/sa/20100115_First_Heatwave_SA_Jan.shtml (accessed Nov. 16, 2021).

[15] 'Värmebölja |SMHI'. http://www.smhi.se/kunskapsbanken/klimat/varmeboljа-1.22372 (accessed Nov. 16, 2021).

[16] 'ΕΜΥ, Εθνική Μετεωρολογική Υπηρεσία'. http://www.emy.gr/emy/el/ (accessed Nov. 16, 2021).

[17] J. A. López-Bueno *et al.*, 'Evolution of the threshold temperature definition of a heat

wave vs. evolution of the minimum mortality temperature: a case study in Spain during the 1983–2018 period', *Environ. Sci. Eur.*, vol. 33, no. 1, p. 101, Aug. 2021, doi: 10.1186/s12302-021-00542-7.

[18] P. J. Robinson, 'On the Definition of a Heat Wave', *J. Appl. Meteorol. Climatol.*, vol. 40, no. 4, pp. 762–775, Apr. 2001, doi: 10.1175/1520-0450(2001)040<0762:OTDOAH>2.0.CO;2.

[19] A. Machard, C. Inard, J.-M. Alessandrini, C. Pelé, and J. Ribéron, 'A Methodology for Assembling Future Weather Files Including Heatwaves for Building Thermal Simulations from the European Coordinated Regional Downscaling Experiment (EURO-CORDEX) Climate Data', *Energies*, vol. 13, no. 13, Art. no. 13, Jan. 2020, doi: 10.3390/en13133424.

[20] C. Zhang, 'Seminar om Ventilation, Indeklima og Energi', p. 13.

[21] N. A. Phillips, 'The general circulation of the atmosphere: A numerical experiment', *Q. J. R. Meteorol. Soc.*, vol. 82, no. 352, pp. 123–164, 1956, doi: 10.1002/qj.49708235202.

[22] N. O. and A. A. US Department of Commerce, 'Breakthrough article on the First Climate Model'.
https://celebrating200years.noaa.gov/breakthroughs/climate_model/welcome.html (accessed Sep. 08, 2021).

[23] F. Giorgi, 'CLIMATE CHANGE PREDICTION', p. 27.

[24] R. M. Trigo and J. P. Palutikof, 'Precipitation Scenarios over Iberia: A Comparison between Direct GCM Output and Different Downscaling Techniques', *J. Clim.*, vol. 14, no. 23, pp. 4422–4446, Dec. 2001, doi: 10.1175/1520-0442(2001)014<4422:PSOIAC>2.0.CO;2.

[25] T. Kershaw, M. Eames, and D. Coley, 'Assessing the risk of climate change for buildings: A comparison between multi-year and probabilistic reference year simulations', *Build. Environ.*, vol. 46, no. 6, pp. 1303–1308, Jun. 2011, doi: 10.1016/j.buildenv.2010.12.018.

[26] 'WG1AR5_Chapter09_FINAL.pdf'. Accessed: Mar. 25, 2021. [Online]. Available: https://www.ipcc.ch/site/assets/uploads/2018/02/WG1AR5_Chapter09_FINAL.pdf

[27] F. Giorgi, 'Thirty Years of Regional Climate Modeling: Where Are We and Where Are We Going next?', *J. Geophys. Res. Atmospheres*, vol. 124, no. 11, pp. 5696–5723, 2019, doi: https://doi.org/10.1029/2018JD030094.

[28] O. Lhotka, J. Kyselý, and E. Plavcová, 'Evaluation of major heat waves' mechanisms in EURO-CORDEX RCMs over Central Europe', *Clim. Dyn.*, vol. 50, no. 11–12, pp. 4249–4262, Jun. 2018, doi: 10.1007/s00382-017-3873-9.

[29] M. F. Jentsch, P. A. B. James, L. Bourikas, and A. S. Bahaj, 'Transforming existing weather data for worldwide locations to enable energy and building performance simulation under future climates', *Renew. Energy*, vol. 55, pp. 514–524, Jul. 2013, doi: 10.1016/j.renene.2012.12.049.

[30] A. Moazami, V. M. Nik, S. Carlucci, and S. Geving, 'Impacts of future weather data typology on building energy performance – Investigating long-term patterns of climate change and extreme weather conditions', *Appl. Energy*, vol. 238, pp. 696–720, Mar. 2019, doi: 10.1016/j.apenergy.2019.01.085.

[31] R. K. Pachauri, L. Mayer, and Intergovernmental Panel on Climate Change, Eds., *Climate change 2014: synthesis report*. Geneva, Switzerland: Intergovernmental Panel on Climate Change, 2015.

[32] I. P. on C. Change, I. P. on C. C. W. G. I, and W. M. Organization, *Climate Change 1992*. Cambridge University Press, 1992.

[33] IPCC, Ed., *Emissions scenarios: summary for policymakers;a special report of IPCC Working Group III$Intergovernmental Panel on Climate Change*. Intergovernmental Panel on

Climate Change, 2000.

[34] M. Meinshausen *et al.*, 'The RCP greenhouse gas concentrations and their extensions from 1765 to 2300', *Clim. Change*, vol. 109, no. 1–2, pp. 213–241, Nov. 2011, doi: 10.1007/s10584-011-0156-z.

[35] P. Friedlingstein *et al.*, 'Global Carbon Budget 2019', *Earth Syst. Sci. Data*, vol. 11, no. 4, pp. 1783–1838, Dec. 2019, doi: 10.5194/essd-11-1783-2019.

[36] D. Jacob *et al.*, 'EURO-CORDEX: new high-resolution climate change projections for European impact research', *Reg. Environ. Change*, vol. 14, no. 2, pp. 563–578, Apr. 2014, doi: 10.1007/s10113-013-0499-2.

[37] F. Kreienkamp, H. Huebener, C. Linke, and A. Spekat, 'Good practice for the usage of climate model simulation results - a discussion paper', *Environ. Syst. Res.*, vol. 1, no. 1, p. 9, 2012, doi: 10.1186/2193-2697-1-9.

[38] F. Giorgi, C. Jones, and G. R. Asrar, 'Addressing climate information needs at the regional level: the CORDEX framework', p. 9.

[39] J. H. Christensen, F. Boberg, O. B. Christensen, and P. Lucas-Picher, 'On the need for bias correction of regional climate change projections of temperature and precipitation', *Geophys. Res. Lett.*, vol. 35, no. 20, 2008, doi: 10.1029/2008GL035694.

[40] J. H. Christensen and F. Boberg, 'Temperature dependent climate projection deficiencies in CMIP5 models', *Geophys. Res. Lett.*, vol. 39, no. 24, 2012, doi: 10.1029/2012GL053650.

[41] J. H. Christensen, E. Kjellström, F. Giorgi, G. Lenderink, and M. Rummukainen, 'Weight assignment in regional climate models', *Clim. Res.*, vol. 44, no. 2–3, pp. 179–194, Dec. 2010, doi: 10.3354/cr00916.

[42] J. W. Spencer, 'A comparison of methods for estimating hourly diffuse solar radiation from global solar radiation', *Sol. Energy*, vol. 29, no. 1, pp. 19–32, Jan. 1982, doi: 10.1016/0038-092X(82)90277-8.

[43] J. Boland, B. Ridley, and B. Brown, 'Models of diffuse solar radiation', *Renew. Energy*, vol. 33, no. 4, pp. 575–584, Apr. 2008, doi: 10.1016/j.renene.2007.04.012.

[44] C. Teutschbein and J. Seibert, 'Is bias correction of regional climate model (RCM) simulations possible for non-stationary conditions?', *Hydrol. Earth Syst. Sci.*, vol. 17, no. 12, pp. 5061–5077, Dec. 2013, doi: 10.5194/hess-17-5061-2013.

[45] A. J. Cannon, 'Multivariate quantile mapping bias correction: an N-dimensional probability density function transform for climate model simulations of multiple variables', *Clim. Dyn.*, vol. 50, no. 1–2, pp. 31–49, Jan. 2018, doi: 10.1007/s00382-017-3580-6.

[46] F. Pitié, A. C. Kokaram, and R. Dahyot, 'Automated colour grading using colour distribution transfer', *Comput. Vis. Image Underst.*, vol. 107, no. 1, pp. 123–137, Jul. 2007, doi: 10.1016/j.cviu.2006.11.011.

[47] R. Mehrotra and A. Sharma, 'A Multivariate Quantile-Matching Bias Correction Approach with Auto- and Cross-Dependence across Multiple Time Scales: Implications for Downscaling', *J. Clim.*, vol. 29, no. 10, pp. 3519–3539, May 2016, doi: 10.1175/JCLI-D-15-0356.1.

[48] A. J. Cannon, 'Multivariate Bias Correction of Climate Model Output: Matching Marginal Distributions and Intervariable Dependence Structure', *J. Clim.*, vol. 29, no. 19, pp. 7045–7064, Oct. 2016, doi: 10.1175/JCLI-D-15-0679.1.

[49] 'Bias Correction of GCM Precipitation by Quantile Mapping: How Well Do Methods Preserve Changes in Quantiles and Extremes? in: Journal of Climate Volume 28 Issue 17

(2015)'. Accessed: Mar. 26, 2021. [Online]. Available: https://journals.ametsoc.org/view/journals/clim/28/17/jcli-d-14-00754.1.xml

[50] A. J. Cannon, 'Multivariate quantile mapping bias correction: an N-dimensional probability density function transform for climate model simulations of multiple variables', *Clim. Dyn.*, vol. 50, no. 1, pp. 31–49, Jan. 2018, doi: 10.1007/s00382-017-3580-6.

[51] D. B. Crawley and C. S. Barnaby, 'Weather and climate in building performance simulation', in *Building Performance Simulation for Design and Operation*, 2nd ed., Routledge, 2019.

[52] National Climatic Center (U.S.), Ed., *Typical meteorological year user's manual TD-9734: hourly solar radiation/surface meteorological observations*. Asheville, N.C: National Climatic Center, 1981.

[53] W. Marion and K. Urban, 'User's Manual for TMY2s Typical Meteorological Years Derived from the 1961-1990 National Solar Radiation Data Base', p. 56.

[54] 'ISO15927-4:2005',*ISO*. https://www.iso.org/cms/render/live/en/sites/isoorg/contents/data/standard/04/13/41371.html (accessed Sep. 06, 2021).

[55] D. R. Easterling, G. A. Meehl, C. Parmesan, S. A. Changnon, T. R. Karl, and L. O. Mearns, 'Climate Extremes: Observations, Modeling, and Impacts', *Science*, Sep. 2000, Accessed: Sep. 03, 2021. [Online]. Available: https://www.science.org/doi/abs/10.1126/science.289.5487.2068

[56] G. A. Meehl, 'More Intense, More Frequent, and Longer Lasting Heat Waves in the 21st Century', *Science*, vol. 305, no. 5686, pp. 994–997, Aug. 2004, doi: 10.1126/science.1098704.

[57] C. Schär *et al.*, 'The role of increasing temperature variability in European summer heatwaves', *Nature*, vol. 427, no. 6972, pp. 332–336, Jan. 2004, doi: 10.1038/nature02300.

[58] G. Ouzeau, J.-M. Soubeyroux, M. Schneider, R. Vautard, and S. Planton, 'Heat waves analysis over France in present and future climate: Application of a new method on the EURO-CORDEX ensemble', *Clim. Serv.*, vol. 4, pp. 1–12, Dec. 2016, doi: 10.1016/j.cliser.2016.09.002.

[59] J. Díaz *et al.*, 'Mortality attributable to high temperatures over the 2021–2050 and 2051–2100 time horizons in Spain: Adaptation and economic estimate', *Environ. Res.*, vol. 172, pp. 475–485, May 2019, doi: 10.1016/j.envres.2019.02.041.

[60] A. Casanueva *et al.*, 'Overview of Existing Heat-Health Warning Systems in Europe', *Int. J. Environ. Res. Public. Health*, vol. 16, no. 15, Art. no. 15, Jan. 2019, doi: 10.3390/ijerph16152657.

[61] B. G. Armstrong *et al.*, 'Association of mortality with high temperatures in a temperate climate: England and Wales', *J. Epidemiol. Community Health*, vol. 65, no. 4, pp. 340–345, Apr. 2011, doi: 10.1136/jech.2009.093161.

[62] 'mn80_theory.pdf'. Accessed: Sep. 06, 2021. [Online]. Available: https://meteonorm.com/assets/downloads/mn80_theory.pdf

[63] C. Y. Siu and Z. Liao, 'Is building energy simulation based on TMY representative: A comparative simulation study on doe reference buildings in Toronto with typical year and historical year type weather files', *Energy Build.*, vol. 211, p. 109760, Mar. 2020, doi: 10.1016/j.enbuild.2020.109760.

ISSN 1901-726X
DCE Technical Report No. 300